Computational study of the influence of callus porosity on ultrasound propagation in healing bones

Vassiliki T. Potsika, Ioannis F. Spiridon, Vasilios C. Protopappas, *Member, IEEE,* Maria G. Vavva, Panagiotis D. Lymperopoulos, Christos V. Massalas, Demosthenes K. Polyzos, Dimitrios I. Fotiadis, *Senior Member, IEEE*

***Abstract*—In the process of fracture healing, several phases of recovery are observed as the mechanical stability, continuity and normal load carrying capacity are gradually restored. The ultrasonic monitoring and discrimination of different healing stages is a complex process due to the significant microstructure and porous nature of osseous and callus tissues. In this study, we investigate the influence of the callus pores' size and concentration on ultrasound propagation in a long bone at a late healing stage. Different excitation frequencies are applied in the range of 300 kHz – 1 MHz. A 2D geometry is developed and axial transmission calculations are performed based on a Finite Element Method. The velocity of the first arriving signal (FAS) and the propagation of guided waves are used as the estimated parameters. It was shown that the FAS velocity can reflect callus porosity changes, while the propagation of guided waves is sensitive to pores' distribution for higher frequencies.**

I. Introduction

Nowadays, quantitative ultrasound is considered as a promising technique for the diagnosis and monitoring of bone pathologies. However, the significant nonhomogeneous and porous nature of bone induces multiple scattering phenomena which cannot be estimated experimentally. To this end, several research groups have performed numerical simulations of ultrasound propagation in osteoporotic and healing bones in order to provide supplementary information to experimental findings and give insight to complex ultrasound propagation phenomena [1–12].

Concerning the ultrasonic evaluation of the bone healing process, the velocity and attenuation of the first arriving signal (FAS) have been used as the main estimated parameters [1–12]. It was observed that the FAS velocity and attenuation depend on the plate thickness and fracture geometry [3–6]. Also, in [2–6] the FAS velocity was shown to decrease during the first healing stages and to increase as the material and geometrical properties are gradually restored. Additionally, in [7, 10, 11], the propagation of guided waves was investigated as an advanced monitoring means of bone healing. It was found that bone anisotropy and geometry irregularity, as well as the material and geometrical changes of callus influence the propagation of guided waves. On the other hand, the FAS velocity was not affected by the irregularity and anisotropy of bone.

More recently, the research interest has been focused on the development of more realistic computational models of fractured long bones based on imaging techniques [13–15] and analytical methods [10, 12, 16]. Scanning acoustic microscopy (SAM) and micro-computed tomography are the most popular imaging techniques that can provide material and geometrical properties of the tissues with spatial resolution within the micrometer range. In [7, 14] the porosity distribution of callus was examined at different healing stages using SAM. A decrease of callus porosity was observed as healing progressed, while the cortical porosity was found to increase [14]. Moreover, wave dispersion and attenuation estimations showed that the role of scattering, material dispersion and absorption phenomena is more significant during the early healing stages [7, 16].

In this study, we present computational models of a healing bone corresponding to a late healing stage to investigate the influence of different pores' sizes and concentrations on ultrasound propagation. For investigating the influence of porosity alone on wave propagation, we made comparisons with cases of cortical plates with different levels of porosity. Calculations of the FAS velocity and the propagation of guided waves are performed for different excitation frequencies. It was found that for all frequencies the FAS velocity is significantly influenced by the porosity distribution, while the features of guided waves depend on the excitation frequency.

II. Materials And Methods

A. Model Geometry

The geometry and the material properties of the computational models were derived from [7] and correspond to a healing bone at the 9th week of consolidation from an animal study [14]. The cortical bone thickness was 4 mm

V. T. Potsika, I. F. Spiridon, V. C. Protopappas are with the Unit of Medical Technology and Intelligent Information Systems, University of Ioannina, GR 45110 Ioannina, Greece (e-mail: vpotsika@gmail.com, spiridon@cc.uoi.gr, vprotopappas@gmail.com).

M. G. Vavva and D. K. Polyzos are with the Department of Mechanical Engineering and Aeronautics, University of Patras, GR 26 500 Patras, Greece (e-mail: marvavva@gmail.com, polyzos@mech.upatras.gr).

P. D. Lymperopoulos is with the Department of Mechanical, Material and Aerospace Engineering, Armour College of Engineering, Illinois Institute of Technology (IIT), Chicago, IL 60616-3793, USA (email: plympero@hawk.iit.edu).

C. V. Massalas is Professor Emeritus at the Dept. of Materials, Science and Engineering, University of Ioannina (email: cmasalas@cc.uoi.gr).

D. I. Fotiadis is with the Unit of Medical Technology and Intelligent Information Systems, University of Ioannina, GR 45110, Ioannina, Greece, and with the Foundation for Research and Technology-Hellas (FORTH) (phone: Another significant conclusion was 0030-2651008803; fax: 00302651008889; email: fotiadis@cs.uoi.gr).

978-1-4244-7929-0/14/$26.00 ©2014 IEEE

and the callus region 3 mm. Callus was considered as a composite medium consisted of a matrix material including spherical blood scatterers. The scatterers were randomly distributed in the callus region. Two series of calculations were performed. In the 1st series (Fig. 1a), cortical bone was considered as a compact medium and five cases were examined for different callus porosity distributions : i) callus porosity 0% (Problem I), ii) callus porosity 22.70 %, pores' diameter 120 μm (Problem II), iii) callus porosity 22.70 %, pores' diameter 240 μm (Problem III), iv) callus porosity 11.35%, pores' diameter 120 μm (Problem IV), v) callus porosity 11.35 %, pores' diameter 240 μm (Problem V). In the 2nd series (Fig. 2b), the callus region was ignored and cortical bone was all considered as a composite medium with blood scatterers with: i) porosity 11.35%, pores' diameter 120 μm (Problem VI), ii) porosity 11.35%, pores' diameter 240 μm (Problem VII). This series was used in order to analyze the influence of porosity alone on the characteristics of wave propagation. The case of intact bone was also considered. Table I summarizes the material properties assigned to cortical bone, callus and blood.

B. Ultrasound Configuration

Concerning Problems I-V, axial-transmission calculations were performed by placing one transmitter and one receiver on each side of the fracture gap directly onto the cortical bone surface. The transducers' size was set to 2 mm, their center-to-center distance was 25 mm and they operated in the longitudinal mode. The same configuration was used for Problems VI-VII. Fig. 1 presents the ultrasound configuration for the two series of calculations.

C. Boundary Conditions

Absorption elements were considered at the ends of cortical bone to simulate an infinitely long plate and neglect reflection from the boundaries.

D. Numerical Simulation and Signal Analysis in the Time Domain

The numerical solution of the 2D wave propagation problem was carried out using the Finite Element Method. In order to describe the propagation of ultrasonic waves in plates, a model of forced vibration was used:

$$[M]\{\ddot{u}\}+[D]\{\dot{u}\}+[K]\{u\}=\{P(t)\} \quad (1)$$

where $[M]$ is the mass matrix, [D] is the dumping matrix, $[K]$ is the stiffness matrix, $\{\ddot{u}\}$ is the acceleration vector, $\{\dot{u}\}$ is the velocity vector, $\{u\}$ is the nodal displacement vector of the particles and $\{P(t)\}$ is the vector of the excitation force [18].

A triangular element type was selected to achieve a reasonable time and memory cost, and the element size was set to $l < \lambda/10$, in which λ is the wavelength. Also, 512 equal timesteps were applied according to the criterion: $\Delta t \le 1/(10\times f)$, in which f denotes the central frequency.

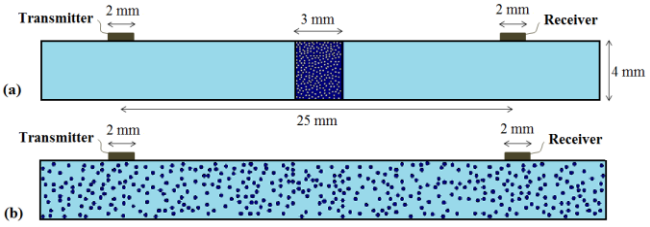

Fig. 1. Ultrasound configuration for: a) the 1st series of calculations (Problem II), the 2nd series of calculations (Problem VII).

These restrictions were applied to acquire a stable analysis, conformed to the Courant–Friedrichs–Lewy condition.

A Hanning sine pulse was used as the excitation signal. The examined central angular frequencies were 300 kHz, 500 kHz and 1 MHz for the 1st series of calculations and the excitation signal included four sinusoidal cycles in the pulse. The central frequencies of 300 kHz and 500 kHz were also examined in the 2nd series of calculations. The duration of the simulated signals recording was 30 μs. In order to detect the FAS a threshold was used, corresponding to the detection of the first signal extremum.

E. Analysis of the propagation of guided waves

All the measured waveforms were subjected to time-frequency (t, f) analysis in order to investigate the influence of the callus and cortical porosity distribution on the propagation of guided waves. The Reassigned Smoothed-Pseudo Wigner-Ville (RSPWV) distribution was used and frequency-group velocity (f, c_g) dispersion curves were calculated for the plate model based on the Lamb wave theory [6, 7]. For all the examined problems and excitation frequencies the (f, c_g) dispersion curves were superimposed to the (t, f) representations. In Fig. 3, analytically derived Lamb dispersion curves of the first three symmetric (denoted as S0, S1, S2) and antisymmetric modes (denoted as A0, A1, A2) are illustrated corresponding to excitation frequency 1 MHz for the 1st series of calculations.

III. Results

Fig. 2 presents the FAS velocity calculations for the 1st series of calculations corresponding to a healing bone. The highest FAS velocity measurements were observed for Problem I corresponding to the case of a homogeneous callus region. On the other hand, the lowest FAS velocity values were measured for Problems II and III corresponding to the highest porosity concentrations. It is also shown that the velocity values computed for Problems II and III, as well as for problems IV and V approximately coincide.

Concerning the frequency dependence of ultrasound propagation, the lowest FAS velocity values were calculated

TABLE I. MATERIAL PROPERTIES

	Bone	Callus	Blood
ρ (kg/m^3)	2016.2	1881.1	1055
E (GPa)	30.3	21.1	0.003
λ (GPa)	17.5	12.2	2.63
μ (GPa)	11.7	8.1	0

for the central frequency of 300 kHz, while the highest values were observed for 1 MHz. Particularly, the FAS velocity calculations were in the range of: i) 2884 – 2944 m/s for 300 kHz, ii) 3227 – 3308 m/s for 500 kHz, iii) 3547 – 3634 m/s for 1 MHz. All calculations were lower in comparison to the case of intact bone.

The RSPWV distributions of the signals obtained by using an excitation frequency of 1 MHz are illustrated in Fig. 3, in which we have also superimposed the dispersion curves of Lamb modes. The symmetric modes (S0, S1, S2) are illustrated with a solid, white line, while the antisymmetric modes (A0, A1, A2) with a dashed, white line. The modes S2 and A1 are seen in all images, whereas the A2 mode is clearly observed in only in the cases of Problem I and intact bone showing a different energy distribution in comparison to other examined problems. Different observations were made for the other excitation frequencies which are not illustrated herein. Specifically, for excitation frequency 300 kHz the lower order modes A0 and A1 were mainly detected in all the examined problems showing no significant differences for different porosity distributions. Also, similar findings were observed for excitation frequency 500 kHz in which the S0 and A1 modes were the dominant modes.

In the 2nd series of calculations, FAS velocity was: a) 2777 m/s for Problem VI and 2701 m/s for Problem VII for excitation frequency 300 kHz, b) 3035 m/s for Problem VI and 3004 m/s for Problem VII for excitation frequency 500 kHz, showing an about 10% decrease compared to the intact cases of the same frequency, whereas the change of the sphere radius, for a specific frequency, had an influence less than 2%. Similar features were observed for the RSPWV distributions of the signals derived for Problems VI and VII (not shown in Figs. herein). Specifically, for excitation frequency 300 kHz the A1 was the dominant mode in both examined problems, while the S0 mode was mainly detected for excitation frequency 500 kHz.

IV. Discussion

In the present study, we investigated the influence of the callus pores' size and concentration on the propagation of ultrasonic waves in a healing long bone. A simple 2D geometry was developed in which callus was considered as a composite medium consisted of a matrix with spherical scatterers. For comparison purposes the influence of cortical

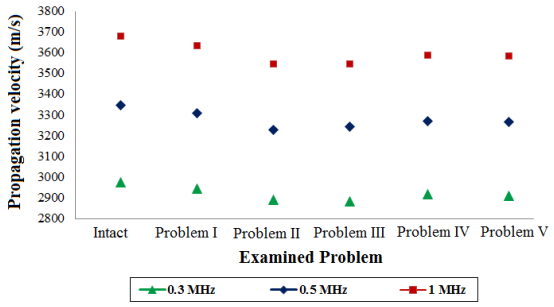

Fig. 2. FAS velocity calculations for different callus porosity distributions and frequencies.

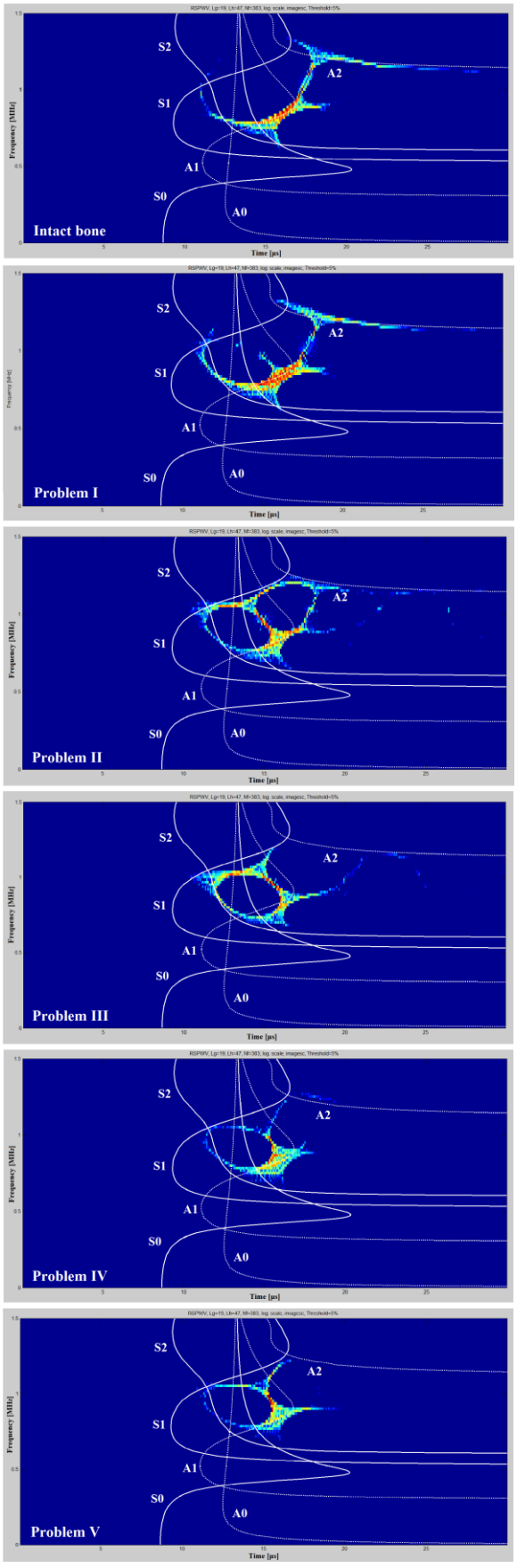

Fig. 3. The RSPWV distribution of the signals obtained for intact bone and Problems I-IV. Central frequency of 1MHz.

porosity on wave propagation was also investigated. FAS velocity calculations and analysis of the propagation of guided waves were performed for different frequencies and porosity distributions of cortical bone and callus so as to give insight to the multiple scattering phenomena occurring at deeper layers of bone and determine quantitatively the interaction of ultrasound with the microstructure of callus.

It was shown that the FAS velocity increases with increasing frequency, which is in agreement with our previous findings [10]. Moreover, the highest FAS velocity values were measured in the case of Problem I corresponding to a homogeneous callus region. This is attributed to the presence of the spherical scatterers which provokes the attenuation of the signal, increasing thus the time of arrival at the receiver. Also, this is reasonable as the propagation velocity in blood is lower in comparison to the callus tissue. Higher FAS velocity values were observed for lower porosity concentrations (Problem IV, V), which however remained lower in comparison to Problem I.

Another significant conclusion was drawn for Problems II and III, as well as Problems IV and V, having the same porosity concentration and different pores' diameters. In these cases, FAS velocity calculations were approximately the same. This reveals that changes in callus porosity concentration have a more significant influence on the propagation of the FAS velocity in comparison to changes in the diameter of the scatterers. Nevertheless, FAS velocity calculations for Problems VI and VII revealed that the scatterers' diameter plays a key role on FAS velocity when larger porous areas are examined such as the whole surface of cortical bone.

Guided wave analysis was also presented for different excitation frequencies. More particularly, for the excitation frequency of 1 MHz it was shown that for Problem I the S2, A2 and A1 are clearly detected in comparison to the other examined problems. On the other hand, for lower excitation frequencies the guided wave propagation features remained almost the same, despite the changes in callus porosity distribution. This indicates that higher frequencies should be applied to study scattering and absorption phenomena in media with significant microstructure such as a healing bone.

However, the assumption that a healing bone is an isotropic, 2D medium is not realistic. Moreover, the same diameter was assigned to the scatterers and the influence of porosity distribution on ultrasound propagation was investigated only for the case of one single healing bone. In our future study, different healing stages will be examined.

V. Conclusions

In this work, we presented 2D simulations of wave propagation in a healing long bone for different porosity distributions and frequencies. Therefore, it could be regarded as a starting point for the future interpretation of FAS velocity measurements and guided wave propagation in more realistic, inhomogeneous and anisotropic numerical models of healing bones.

References

[1] V.C. Protopappas, D.I. Fotiadis, and K.N. Malizos, "Guided Ultrasound wave propagation in intact and healing long bones," *Ultrasound in Med. & Biol.,* vol. 32, pp. 693–708, 2006.

[2] M.G. Vavva, V.C. Protopappas, L.N. Gergidis, A. Charalambopoulos, D.I. Fotiadis, and D. Polyzos, "Velocity dispersion of guided waves propagating in a free gradient elastic plate: Application to cortical bone," *J. Accoust. Soc. Am.,* vol. 125, pp. 3414–3427, 2009.

[3] C.B. Machado, W.C. de Albuquerque Pereira, M. Granke, M. Talmant, F. Padilla, and P. Laugier, "Experimental and simulation results on the effect of cortical bone mineralization measurements: A model for fracture healing ultrasound monitoring," *Bone*, vol. 48, pp. 1202–1209, 2011.

[4] C.B. Machado, W.C. de Albuquerque Pereira, M. Talmant, F. Padilla, and P. Laugier, "Computational evaluation of the compositional factors in fracture healing affecting ultrasound axial transmission measurements," *Ultrasound in Med. & Biol*., pp. 1314–1326, 2010.

[5] S.P. Dodd, J.L. Cunningham, A.W. Miles, S. Gheduzzi, and V.H. Humphrey, "Ultrasound transmission loss across transverse and oblique bone fractures: an in vitro study," *Ultrasound in Med. & Biol*., vol. 34, pp. 454–462, 2008.

[6] V.C. Protopappas, I.C. Kourtis, and L.C. Kourtis, K.N. Malizos, C.V. Massalas, and D.I. Fotiadis, "Three dimensional finite element modeling of guided ultrasound wave propagation in intact and healing long bones," *J. Accoust. Soc. Am.,* vol. 121, pp. 3907–3921, 2007.

[7] V.T. Potsika, K.N. Grivas, V.C. Protopappas, M.G. Vavva, K. Raum, D. Rohrbach, D. Polyzos, D.I. Fotiadis, "Application of an effective medium theory for modeling ultrasound wave propagation in healing long bones," *Ultrasonics*, 2013.

[8] K. Rohde, D. Rohrbach, C.-C. Gluer, P. Laugier, Q. Grimal, K. Raum, R. Barkmann, "Influence of Porosity, Pore Size, and Cortical Thickness on the Propagation of Ultrasonic Waves Guided Through the Femoral Neck Cortex: A Simulation Study," *IEEE Transactions on Ultrasonics, Ferroelectrics, and Frequency Control,* vol. 61, pp. 302–313, 2014.

[9] D. Rohrbach, J. Grondin, Q. Grimal, P. Laugier, R. Barkmann, and K. Raum, "Evidence based numerical ultrasound simulations at the human femoral neck," *Biomed. Tech.*, suppl. 1, pp. 240–243, 2010.

[10] V.T. Potsika, V.C. Protopappas, M.G. Vavva, K. Raum, D. Rohrbach, D. Polyzos, D. I. Fotiadis, "Two-dimensional simulations of wave propagation in healing long bones based on scanning acoustic microscopy images," *International Ultrasonics Symposium*, Dresden, 2012.

[11] M.G. Vavva, V.C. Protopappas, L.N. Gergidis, A. Charalambopoulos, D.I. Fotiadis, D. Polyzos, "The effect of boundary conditions on guided wave propagation in two-dimensional models of healing bone," *Ultrasonics*, pp.598–606, 2008.

[12] A. Papacharalampopoulos, M.G. Vavva, V.C. Protopappas, D.I. Fotiadis, D. Polyzos, "A numerical study on the propagation of Rayleigh and guided waves in cortical bone according to Mindlin's Form II gradient elastic theory," *J. Acoust. Soc. Am*., pp. 1060–1070, 2011.

[13] D. Rohrbach, B. Preininger, B. Hesse, H. Gerigk, C. Perka, K. Raum, "The Early Phases of Bone Healing Can Be Differentiated in a Rat Osteotomy Model by Focused Transverse-Transmission Ultrasound," *Ultrasound Med Biol.,* pp. 1642-53,2013.

[14] B. Preininger, S. Checa, F.L. Molnar, P. Fratzl, G.N. Duda, K. Raum, "Spatial-temporal mapping of bone structural and elastic properties in a sheep model following osteotomy," *Ultrasound in Med. & Biol*., pp. 474–483, 2011.

[15] K. Raum, R.O. Cleveland, F. Peyrin, and P. Laugier, "Derivation of elastic stiffness from site-matched mineral density and acoustic impedance," *Phys. Med. Biol*., pp. 747–758, 2006.

[16] G. Aggelis, S.V. Tsinopoulos, and D. Polyzos, "An iterative effective medium approximation for wave dispersion and attenuation predictions in particulate composites, suspensions and emulsions" *J.* Acoust. Soc. Am., vol. 9, pp. 3443-3452, 2004.

[17] P. Laugier, G. Haiat, Bone Qualitative Ultrasound, Springer, 2011.

[18] R. Courant, K. Friedrichs und H. Lewy, Uber die partiellen Differenzengleiehungen der mathematisehen Physik, Mathematische Annalen, vol. 100, pp. 32-74, 1928.